doi:10.1093/brain/awx195 BRAIN 2017: 140; 2322–2336 | 2322

BRAIN
A JOURNAL OF NEUROLOGY

Delineating *SPTAN1* associated phenotypes: from isolated epilepsy to encephalopathy with progressive brain atrophy

Steffen Syrbe,[1,*] Frederike L. Harms,[2,*] Elena Parrini,[3] Martino Montomoli,[3] Ulrike Mütze,[1] Katherine L. Helbig,[4] Tilman Polster,[5] Beate Albrecht,[6] Ulrich Bernbeck,[7] Ellen van Binsbergen,[8] Saskia Biskup,[9] Lydie Burglen,[10,11] Jonas Denecke,[12] Bénédicte Heron,[11,13] Henrike O. Heyne,[14] Georg F. Hoffmann,[1] Frauke Hornemann,[15] Takeshi Matsushige,[16] Ryuki Matsuura,[17] Mitsuhiro Kato,[18] G. Christoph Korenke,[19] Alma Kuechler,[6] Constanze Lämmer,[20] Andreas Merkenschlager,[15] Cyril Mignot,[21,22] Susanne Ruf,[23] Mitsuko Nakashima,[24] Hirotomo Saitsu,[25] Hannah Stamberger,[26,27,28] Tiziana Pisano,[3] Jun Tohyama,[29] Sarah Weckhuysen,[26,27,28] Wendy Werckx,[30] Julia Wickert,[2,†] Francesco Mari,[3] Nienke E. Verbeek,[8] Rikke S. Møller,[31,32] Bobby Koeleman,[8] Naomichi Matsumoto,[24] William B. Dobyns,[33,34] Domenica Battaglia,[35] Johannes R. Lemke,[14,#] Kerstin Kutsche[2,#] and Renzo Guerrini[3,36,#]

[*,#]These authors contributed equally to this work.

De novo in-frame deletions and duplications in the *SPTAN1* gene, encoding the non-erythrocyte αII spectrin, have been associated with severe West syndrome with hypomyelination and pontocerebellar atrophy. We aimed at comprehensively delineating the phenotypic spectrum associated with *SPTAN1* mutations. Using different molecular genetic techniques, we identified 20 patients with a pathogenic or likely pathogenic *SPTAN1* variant and reviewed their clinical, genetic and imaging data. *SPTAN1 de novo* alterations included seven unique missense variants and nine in-frame deletions/duplications of which 12 were novel. The recurrent three-amino acid duplication p.(Asp2303_Leu2305dup) occurred in five patients. Our patient cohort exhibited a broad spectrum of neurodevelopmental phenotypes, comprising six patients with mild to moderate intellectual disability, with or without epilepsy and behavioural disorders, and 14 patients with infantile epileptic encephalopathy, of which 13 had severe neurodevelopmental impairment and four died in early childhood. Imaging studies suggested that the severity of neurological impairment and epilepsy correlates with that of structural abnormalities as well as the mutation type and location. Out of seven patients harbouring mutations outside the α/β spectrin heterodimerization domain, four had normal brain imaging and three exhibited moderately progressive brain and/or cerebellar atrophy. Twelve of 13 patients with mutations located within the spectrin heterodimer contact site exhibited severe and progressive brain, brainstem and cerebellar atrophy, with hypomyelination in most. We used fibroblasts from five patients to study spectrin aggregate formation by Triton-X extraction and immunocytochemistry followed by fluorescence microscopy. αII/βII aggregates and αII spectrin in the insoluble protein fraction were observed in fibroblasts derived from patients with the mutations p.(Glu2207del), p.(Asp2303_Leu2305dup) and p.(Arg2308_Met2309dup), all falling in the nucleation site of the α/β spectrin heterodimer region. Molecular modelling of the seven *SPTAN1* amino acid changes provided preliminary evidence for structural alterations of the A-, B- and/or C-helices within each of the mutated spectrin repeats. We conclude that *SPTAN1*-related disorders comprise a wide spectrum of neurodevelopmental phenotypes ranging from mild to severe and progressive. Spectrin aggregate formation in fibroblasts with mutations in the α/β heterodimerization domain seems to be associated with a

Received January 19, 2017. Revised May 22, 2017. Accepted June 13, 2017.

severe neurodegenerative course and suggests that the amino acid stretch from Asp2303 to Met2309 in the α20 repeat is important for α/β spectrin heterodimer formation and/or αII spectrin function.

1 Department of General Paediatrics, Division of Child Neurology and Inherited Metabolic Diseases, Centre for Paediatrics and Adolescent Medicine, University Hospital Heidelberg, Heidelberg, Germany
2 Institute of Human Genetics, University Medical Center Hamburg-Eppendorf, Hamburg, Germany
3 Pediatric Neurology, Neurogenetics and Neurobiology Unit and Laboratories, Neuroscience Department, A Meyer Children's Hospital, University of Florence, Florence, Italy
4 Department of Clinical Genomics, Ambry Genetics, Aliso Viejo, California, USA
5 Bethel Epilepsy Center – Krankenhaus Mara GmbH Bielefeld, Germany
6 Institut für Humangenetik, Universitaetsklinikum Essen, Universitaet Duisburg-Essen, Germany
7 Rems-Murr-Kliniken GmbH, Klinik für Kinder- und Jugendmedizin, Winnenden, Germany
8 Department of Genetics, University Medical Center Utrecht, 3508 GA Utrecht, The Netherlands
9 CeGaT-Center for Genomics and Transcriptomics GmbH, Tuebingen, Germany
10 Centre de référence des Malformations et maladies congénitales du cervelet and Département de Génétique et embryologie médicales, AP-HP, GHUEP, Hôpital Trousseau 75012 Paris, France
11 GRC ConCer-LD, Sorbonne Universités, UPMC Univ 06, Paris, France
12 Department of Pediatrics, University Medical Center Hamburg-Eppendorf, Hamburg, Germany
13 AP-HP, Hôpital Trousseau, Service de Neurologie Pédiatrique; Paris, France
14 Institute of Human Genetics, University of Leipzig Hospitals and Clinics, Leipzig, Germany
15 Department of Women and Child Health, Hospital for Children and Adolescents, University of Leipzig Hospitals and Clinics, Leipzig, Germany
16 Department of Pediatrics, Yamaguchi University Graduate School of Medicine, Ube, Japan
17 Division of Neurology, Saitama Children's Medical Center, Saitama, Japan
18 Department of Pediatrics, Showa University School of Medicine, Hatanodai, Shinagawa-ku, Tokyo, Japan
19 Klinikum Oldenburg, Zentrum für Kinder- und Jugendmedizin, Klinik für Neuropaediatrie u. angeborene Stoffwechselerkrankungen, Oldenburg, Germany
20 St. Bernward Krankenhaus, Hildesheim, Germany
21 AP-HP, Département de Génétique and Centre de Référence Déficiences Intellectuelles de Causes Rares, Paris, France
22 GRC UPMC "Déficiences Intellectuelles et Autisme", Groupe Hospitalier Pitié-Salpêtrière, Paris, France
23 Department of Pediatric Neurology and Developmental Medicine, University Children's Hospital, Tübingen, Germany
24 Department of Human Genetics, Yokohama City University Graduate School of Medicine, Yokohama, Japan
25 Department of Biochemistry, Hamamatsu University School of Medicine, Hamamatsu, Japan
26 Neurogenetics Group, Center for Molecular Neurology, VIB, Antwerp, Belgium
27 Laboratory of Neurogenetics, Institute Born-Bunge, University of Antwerp, Belgium
28 Division of Neurology; Antwerp University Hospital, Antwerp, Belgium
29 Department of Pediatrics, Nishi-Niigata Chuo National Hospital, Niigata, Japan
30 Jessa Hospital, Hasselt, Belgium
31 Danish Epilepsy Centre, Dianalund, Denmark
32 Institute for Regional Health Services, University of Southern Denmark, Odense, Denmark
33 Departments of Pediatrics and Neurology, University of Washington, Seattle, Washington, USA
34 Center for Integrative Brain Research, Seattle Children's Research Institute, Seattle, Washington, USA
35 Child Neurology and Psychiatry Unit, Catholic University, Largo Gemelli 18, Rome, Italy
36 IRCCS Stella Maris Foundation, Pisa, Italy

†Present address: Amedes, Human Genetics, Hamburg, Germany

Correspondence to: Dr med. Steffen Syrbe
Department of General Paediatrics, Division of Child Neurology and Inherited Metabolic Diseases, Centre for Paediatrics and Adolescent Medicine, University Hospital Heidelberg, Heidelberg, Germany
E-mail: steffen.syrbe@med.uni-heidelberg.de

Correspondence may also be addressed to: Prof. Renzo Guerrini
Pediatric Neurology, Neurogenetics and Neurobiology Unit and Laboratories, Neuroscience Department, A Meyer Children's Hospital, University of Florence, Florence, Italy
E-mail: r.guerrini@meyer.it

Keywords: epileptic encephalopathy; West syndrome; myoclonic epilepsy; pontocerebellar atrophy; hypomyelination

Abbreviation: EIEE5 = epileptic encephalopathy, early infantile, 5

Introduction

In 2008, four patients exhibiting a distinctive form of early-onset West syndrome with brain hypomyelination and reduced white matter were reported (Tohyama *et al.*, 2008). Subsequently, *de novo* in-frame indels in *SPTAN1*, encoding the non-erythrocyte αII spectrin, were identified in two of them [c.6619_6621del/p.(Glu2207del) and c.6923_6928dup/p.(Arg2308_Met2309dup)] (Saitsu *et al.*, 2010). Both patients had severe developmental delay, spastic quadriplegia, poor visual attention, and distinctive MRI features, including, in addition to hypomyelination, progressive cortical and pontocerebellar atrophy [epileptic encephalopathy, early infantile, 5 (EIEE5), MIM 613477] (Saitsu *et al.*, 2010). Another of the four initially reported patients had a microdeletion of 9q33.3–q34.11 involving *SPTAN1* and *STXBP1* (Tohyama *et al.*, 2008), whose mutations also cause early-onset epileptic encephalopathies, such as Ohtahara or West syndrome (Saitsu *et al.*, 2008).

Fourteen patients with alterations in *SPTAN1* have been reported to date (Supplementary Table 1), including eight patients with EIEE5 carrying *de novo* in-frame duplications or deletions (Saitsu *et al.*, 2010; Hamdan *et al.*, 2012; Writzl *et al.*, 2012; Nonoda *et al.*, 2013; Ream and Mikati, 2014; Tohyama *et al.*, 2015), four with *SPTAN1* missense variants and less defined neurodevelopmental disorders (Hamdan *et al.*, 2012; An *et al.*, 2014; Gilissen *et al.*, 2014; Stavropoulos *et al.*, 2016) and two unrelated individuals with the *de novo* nonsense variant p.(Gln2035*) (Yavarna *et al.*, 2015; Retterer *et al.*, 2016), one of whom with a severe neurodevelopmental disorder, comprising microcephaly, intellectual disability, seizures, hearing and visual loss, agenesis of the corpus callosum, and cerebellar hypoplasia (Yavarna *et al.*, 2015).

α and β spectrins are major components of the membrane skeleton and made up of a succession of spectrin repeats composed of triple helical motifs (α1 to α20 in αII spectrin). Spectrins exist as tetramers composed of antiparallel α and β heterodimers (Machnicka *et al.*, 2014). Heterodimers between mutant αII [p.(Glu2207del) or p.(Arg2308_Met2309dup)] and βII spectrins were less stable than wild-type αII/βII heterodimers, leading to aggregate formation in cultured mouse cortical neurons. Moreover, defective αII/βII and αII/βIII spectrin heterodimers disrupted the cytoskeletal scaffold at the axon initial segment and were associated with an elevated action potential threshold. These data demonstrated that in-frame deletions and duplications affecting one of the two final spectrin repeats required for α/β heterodimerization had a dominant-negative effect on spectrin dimer formation and function (Saitsu *et al.*, 2010). Expression of αII spectrin with the amino acid change p.(Arg566Pro) induced spectrin aggregate formation in a significant proportion of neuroblastoma 2 A (N2A) cells. However, pathogenic relevance of this variant, which was found *de novo* in a patient with mild non-syndromic intellectual disability, still awaits clarification (Hamdan *et al.*, 2012). Spectrins underlie the plasma membrane (Machnicka *et al.*, 2014) and various stimuli can lead to changes in their cellular distribution. For example, in early apoptosis, spectrin aggregation was observed in Jurkat T and HL60 cell lines, which concomitantly changed a portion of spectrin from a soluble to an insoluble protein as it appeared in the Triton™ X-100 insoluble cellular fraction (Dubielecka *et al.*, 2010). On the other hand, proteolysis of αII spectrin is an early event in neural cell pathology (Czogalla and Sikorski, 2005), and calpain and caspase-3 mediated spectrin breakdown products are found in a number of neurodegenerative conditions (Yan *et al.*, 2012). These findings suggest that aggregation or cleavage of αII spectrin may play a role in *SPTAN1* encephalopathy.

We collected data on 20 patients harbouring pathogenic variants in *SPTAN1* with the aim of delineating the associated mutational and clinical spectrum.

Materials and methods

Patients

We recruited patients with pathogenic or likely pathogenic *SPTAN1* variants from different diagnostic and research cohorts from Europe, the USA and Japan. Genetic testing was performed by different approaches, such as single gene sequencing (Patients 8 and 11), targeted panel sequencing (Patients 1, 2, 4–7, 9, 13–15, 17 and 19) (Lemke *et al.*, 2012; Cellini *et al.*, 2016; de Kovel *et al.*, 2016) and whole-exome sequencing (Patients 3, 10, 12, 16, 18, 20) (Saitsu *et al.*, 2013; Kortum *et al.*, 2015; Helbig *et al.*, 2016). The study and genetic testing were performed in accordance with the respective national ethics guidelines and approved by the local authorities in the participating study centres of the University of Leipzig, Germany (224/16-ek), of the Hamburg Medical Chamber (Hamburg, Germany; PV3802), of Yokohama City University School of Medicine, Yokohama, Japan (A140925001), and of Showa University School of Medicine, Tokyo, Japan (H27-219), as well as by the Paediatric Ethics Committees of the Tuscany Region, Italy, in the context of the DESIRE FP7 EU project (see 'Funding' section).

We reviewed clinical, imaging, EEG and genetic information. All patients were studied with repeated EEG recordings while awake and asleep and had at least one brain MRI scan; nine had repeated MRI scans during follow-up. Growth parameters and microcephaly, defined as occipitofrontal circumference below two standard deviation (SD) scores were determined in comparison to country-specific control cohorts. All probands or their parents or legal guardians gave informed consent for genetic testing and/or skin biopsy.

Variant classification

Variants in *SPTAN1* (mRNA reference number: NM_00 1130438) were classified according to established guidelines of the American College of Medical Genetics (ACMG) (Richards *et al.*, 2015). The databases of the 1000 Genomes Project, the Exome Sequencing Project, the Exome Aggregation Consortium (ExAC), The Genome Aggregation Database

(gnomAD), and the Human Genetic Variation Database (HGV) (Higasa *et al.*, 2016) served as control populations (http://www.1000genomes.org/home, http://evs.gs.washington.edu/EVS/, http://exac.broadinstitute.org/, http://gnomad.broadinstitute.org/, http://www.hgvd.genome.med.kyoto-u.ac.jp). For detailed descriptions of the applied sequencing techniques, see the online Supplementary material.

Immunocytochemistry and fluorescence microscopy

Primary fibroblasts of Patients 2, 6, 10, 15 and 17 and one control individual were cultivated on glass coverslips overnight in Dulbecco's modified Eagle medium (DMEM; ThermoFisher) supplemented with 10% foetal bovine serum (FBS; GE Healthcare) and penicillin-streptomycin (100 U/ml and 100 mg/ml, respectively; ThermoFisher). Cells were fixed with 4% paraformaldehyde (Sigma-Aldrich) in phosphate-buffered saline (PBS). After treatment with permeabilization/blocking solution (2% bovine serum albumin; 3% goat serum; 0.5% Nonidet™ P40 in PBS), cells were incubated in antibody solution (3% goat serum; 0.1% Nonidet™ P40 in PBS) containing mouse monoclonal anti-α fodrin antibody (1:400 dilution; clone: D8B7; Abcam), detecting αII spectrin, and rabbit anti-SPTBN1 antibody (1:400; Abcam), detecting βII spectrin. Cells were washed with PBS and incubated with Alexa Fluor® 488 coupled goat anti-mouse IgG (1:1000 dilution; ThermoFisher) and Alexa Fluor® 546 coupled goat anti-rabbit IgG (1:1000 dilution; ThermoFisher). After extensive washing with PBS, cells were embedded in mounting solution (ProLong® Diamond Antifade Mountant with DAPI; ThermoFisher). Cells were analysed with Olympus IX-81 epifluorescence microscope equipped with a 60 × Plan Apo N oil immersion objective lens. Images of patients' and control fibroblasts were taken with the same camera settings [TexasRed (red) 2 s, FITC (green) 300 ms, DAPI (blue) 1 s] and were not subjected to further processing.

Triton™ X extraction

Primary fibroblasts of Patients 2, 6, 10, 15 and 17 and three control individuals were cultivated on 10 cm dishes to 90% confluency and Triton™ X extraction was adapted from (Michalczyk *et al.*, 2016). Briefly, fibroblasts were incubated in a mild lysis buffer [50 mM Tris-HCl (pH 7.5), 150 mM NaCl, 5 mM EDTA and 1% Triton™ X (v/v)] for 10 min on ice. Lysates were cleared by centrifugation for 20 min at 4°C and 30 000 *g*. Sample buffer (33% glycerol; 80 mM Tris-HCl, pH 6.8; 0.3 M dithiothreitol; 6.7% sodium dodecyl sulphate; 0.1% bromophenol blue) was added to supernatant (S) and pellet (P). Both were separated on SDS-PAGE, transferred to PVDF membranes, and subjected to immunodetection. Blots were probed with mouse monoclonal anti-α fodrin antibody (1:1000 dilution; clone: D8B7; Abcam). As a control, blots were analysed using mouse anti-tubulin antibody (1:10 000 dilution; Sigma-Aldrich).

Cleaved αII spectrin assay

Primary fibroblasts of Patients 10 and 17 and two control individuals were cultured in 10% culture medium supplemented with 1 μM staurosporine (Sigma-Aldrich) for 0 h, 4 h, 24 h and 48 h. Every 24 h, medium was changed to fresh 10% culture medium supplemented with 1 μM staurosporine. Cells were lysed in ice-cold RIPA buffer (150 mM NaCl, 1% NP-40, 0.5% sodium deoxycholate, 0.1% SDS, 50 mM Tris, pH 8) supplemented with protease inhibitor cocktail (Roche). Cell lysates were subjected to SDS-PAGE and western blot analysis. Blots were probed with rabbit anti-α fodrin antibody (1:1000 dilution; Cell Signaling), which detects full-length αII spectrin and the cleaved 150 kDa fragment. To control for equal loading, blots were probed with mouse anti-α tubulin antibody.

TUNEL assay

Primary fibroblasts of Patients 10 and 17 and two control individuals were cultivated in 10% culture medium supplemented with 1 μM staurosporine for 0, 48 and 72 h. Cells were trypsinized and a TUNEL assay was performed using the APO-BrdU™ TUNEL Assay Kit (ThermoFisher) according to the manufacturer's instructions. BrdU incorporation was measured by flow cytometry using a FACS Calibur (BD Biosciences). The percentage of BrdU positive cells was determined using CellQuestPro Software (BD Biosciences).

Starvation assay

To induce autophagy, primary fibroblasts of Patients 10 and 17 and two control individuals were incubated in starvation medium (DMEM supplemented with 1% FBS) for 0, 2 and 4 h. Cells were lysed in ice-cold RIPA buffer and lysates were subjected to SDS-PAGE and immunodetection. Blots were analysed with rabbit anti-LC3B/MAP1LC3B antibody (1:1000 dilution; Novusbio) and mouse anti-GAPDH (1:10 000 dilution; Abcam).

The protein level of the autophagy marker beclin 1 was analysed in cell lysates of untreated fibroblasts of Patients 2, 6, 10, 15, and 17 and three control individuals. Cells were harvested and lysates were subjected to SDS-PAGE and immunoblotting. Blots were probed with rabbit monoclonal anti-beclin antibody (1:400 dilution; clone: H-300; Santa Cruz Technology) and mouse anti-GAPDH antibody.

Molecular modelling

The 3D structure of the spectrin repeats of αII spectrin was obtained through homology modelling using the SWISS-MODEL web-based service (Schwede *et al.*, 2003). The crystallographic structure at 2.0-Å resolution of two spectrin repeats (15–16) of brain α-spectrin (PDB entry 1u5p.1.A) was used as a template. The selected template ensured the best sequence identity over all homology modellings (15.95–97.67%). Molecular graphics were developed with UCSF Chimera software (Pettersen *et al.*, 2004). For simulating disease-associated amino acid substitutions and the analysis of steric clashes UCSF Chimera build-in tools were used.

Results

We studied 20 novel patients of whom 18 exhibited a *de novo* *SPTAN1* variant and two (Patients 6 and 7) a

recurrent variant that, although not tested in the parents, had previously been classified as pathogenic (Saitsu *et al.*, 2010) (Fig. 1, Table 1 and Supplementary Table 2). For all patients, detailed clinical data were available to comprehensively delineate the phenotypic spectrum associated with *SPTAN1* mutations.

Phenotypic spectrum

The vast majority of patients in our cohort exhibited epilepsy (19/20; 95%). We classified 14 of 20 patients as having an early infantile epileptic encephalopathy (14/19 with epilepsy, 74%; Table 1). In this group of patients, infantile spasms were the most prominent seizure type (13/14, 93% with epileptic encephalopathy; 13/19, 68% of all patients with epilepsy). Infantile spasms manifested at a median age of 4 months (ranging from neonatal onset to 9 months) and occurred in the context of an infantile epileptic encephalopathy with infantile spasms (2/14 epileptic encephalopathy cases; 14%) or as part of West syndrome (11/14; 79%), in the latter case being accompanied by hypsarrhythmia on EEG. One single infant (Patient 5, 1/14; 7%) presented with tonic seizures. Infantile spasms persisted up to a median age of 3 years (2.5–5.6 years) in five individuals, additional myoclonic, tonic seizures, and focal dyscognitive seizures were reported later in these children. In some patients in this group, hypsarrhythmia on the EEG persisted up to 2–3 years of age (Patients 9 and 13), while in most patients generalized background slowing (6/14, 43%) and multifocal epileptiform potentials (5/14, 36%) were prominent EEG features after infancy (Table 1).

In the 14 patients with epileptic encephalopathy, infantile spasms were highly refractory to treatment and no superior medication was identified. A median number of five (1–11) different antiepileptic drugs (AEDs) were tested. The following treatments had partial or temporary effectiveness on spasms in single patients: vigabatrin, adrenocorticotropic hormone, a combination of vigabatrin + adrenocorticotropic hormone, valproic acid, topiramate, clobazam, pyridoxal 5'-phosphate, levetiracetam and ketogenic diet. The same medications, however, were ineffective in other individuals in this series. Patients 16 and 19 became free of spasms under initial treatment with valproic acid and adrenocorticotropic hormone or vigabatrin, respectively, and developed only mild developmental delay (Table 1).

Three patients (Patients 8, 10 and 14) died unexpectedly between ages 3.6 and 4.3 years, consistent with sudden unexpected death in epilepsy (SUDEP). Patient 13 died from respiratory failure at 5.6 years (Table 1).

Hypotonia was an early sign of abnormal development (11/14 in the group of patients with epileptic encephalopathy, 79%; 13/20, 65% of all). Most individuals with infantile epileptic encephalopathy (12/14, 86%) in this study exhibited profound developmental delay with quadriplegia and absent speech; only two patients (Patients 16 and 19; 14%) acquired communicative and motor skills. Lack of visual contact (10/14, 71%) and movement disorder, such as opisthotonic posturing (2/14, 14%) or dyskinetic movements (3/14, 21%) were additional early findings. Overall, 10/14 (71%; 10/20, 50% of all) individuals exhibited the full picture of the initially described EIEE5 including infantile spasms, poor visual attention and MRI features of cerebellar atrophy and hypomyelination (see 'Neuroimaging data' section). One patient was initially diagnosed with PEHO (progressive encephalopathy with oedema, hypsarrhythmia and optic atrophy) syndrome (Patient 11),

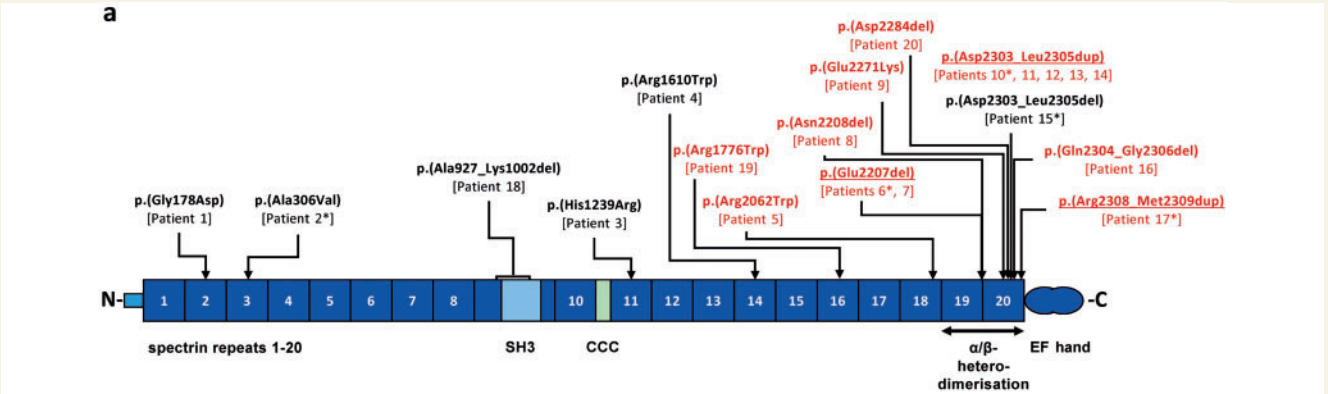

Figure 1 *SPTAN1* variants and domain structure of the encoded αII spectrin. Variants are given in the three-letter code above the schematic of αII spectrin. The known mutations p.(Glu2207del), p.(Asp2303_Leu2305dup), and p.(Arg2308_2309dup) identified in our study are underlined. Novel *SPTAN1* mutations are indicated in black or red based on the severity of the patient's phenotype (red: infantile epileptic encephalopathy; black: childhood onset epilepsy syndromes; Table 1). Patient numbers are indicated below each mutation. Patients for whom fibroblasts were used in this study are marked with an asterisk. α spectrin repeats (α1 to α20) are indicated as dark blue boxes and numbered. The SH3 domain (light blue box) is located within α9 and the CCC (Ca^{2+}-dependent binding site for calmodulin and cleavage sites for caspases and calpain) domain (light green box) within α10. EF hands are indicated as two blue circles at the C-terminus. α19 and α20 repeats are required for α/β heterodimerization (double arrow). N = NH_2-terminus; C = COOH-terminus.

Table 1 Clinical information on 20 patients with *de novo SPTAN1* alterations

Patient/ gender	Age at last follow-up	Mutation	Epilepsy syndrome	Seizure onset	EEG	Seizure outcome	Current treatment (previous medication)	Development; Clinical examination	Brain MRI	OFC at birth/postnatal OFC at last follow-up (SD score)	Reference
Individuals with *de novo* variants in *SPTAN1* and infantile epileptic encephalopathy											
19/F	3 y 6 m	c.5326C>T p.(Arg1776Trp) *De novo*	Infantile EE with IS and focal epilepsy	9 m	Right fronto-temporal SW	Cessation of spasms at 11 m; focal seizures	CBZ (VGB)	Mild ID, ASD; Normal	Normal at 2 y 10 m (Supplementary Fig. 3)	n.a. / 51 cm (+1)	Novel
5/F	3 y	c.6184C>T p.(Arg2062Trp) *De novo*	Infantile EE with tonic spasms and FDS	7 m	Slowing of background activity at 7 m and 1 y 3 m	Persisting FDS and tonic seizures	VPA + LEV	Profound DD, severe hypotonia, lack of visual attention; Microcephaly	Supratentorial atrophy, severe thinning of CC, hypomyelination, at 3 y (Supplementary Fig. 1)	32 cm (−0.65) / 44 cm (−5.1), at 3 y	Novel
6/F	3 y	c.6619_6621del p.(Glu2207del) Parents not tested	West syndrome	2 m	Hypsarrhythmia up to 12 m; at 2 y generalized slow background with posterior spike wave	Ongoing IS - less severe	VGB + CLB (CZP, B6, STM + VGB temporary effect on IS (2 m free of IS), VGB + Pred partially effective on IS	Profound DD, minimal interaction, hypotonia, hypokinesia; Microcephaly	Mild brain/pontocerebellar atrophy, hypomyelination, at 6 m (Supplementary Fig. 1)	33.5 cm (−1.3) / 42 cm (−7), at 3 y	Saitsu *et al.*, 2010
7/F	3 y	c.6619_6621del p.(Glu2207del) Parents not tested	West syndrome	4 m	Hypsarrhythmia, at 3 y background slowing, multifocal ETP	Persisting tonic spasms	LTG + VPA (KD, LEV, CLB, VGB, B6, Pred, STM, TPM)	Profound DD, hypotonia, lack of visual attention; Microcephaly	Cerebellar and brainstem atrophy, thin CC, hypomyelination, at 3 m (Supplementary Fig. 2)	34 cm (−0.5) / 42.1 cm (−6.8), at 2.5 y	Saitsu *et al.*, 2010
8/F	4 y[a]	c.6622_6624del p.(Asn2208del) *De novo*	West syndrome	Neonatal	Hypsarrhythmia at 3 m, background slowing with bifronto-temporal spikes at 7 m, multifocal slow waves and spikes at 3 y	Persisting polymorphic seizures	VPA + VGB (VGB transient effect on IS, Pred, TPM, LEV, PB, Nitrazepam, B6, folinic acid, KD)	Profound DD, severe hypotonia, lack of visual attention, thermic dysregulation; Microcephaly	Global brain, brainstem and cerebellar atrophy, extremely thin CC, hypomyelination, at 2 y (Fig. 2)	35.5 cm (+0.64) / 46 cm (−2), at 4 y	Novel
9/F	3 y	c.6811G>A p.(Glu2271Lys) *De novo*	West syndrome	4 m	Hypsarrhythmia up to 3 y	Persisting subtle IS and tonic seizures	PB + VPA + VGB + Pred (ACTH, LEV, STM, B6, KD)	Profound DD, hypotonia, multifocal myoclonus, dyskinetic movement disorder, lack of visual attention; Microcephaly	Global atrophy, more pronounced on cerebellum / brainstem, thin CC, hypomyelination, at 10 m (Supplementary Fig. 1)	33.5 cm (−0.61) / 42.3 cm (−2), at 10 m	Novel
20/M	3 y	c.6850_6852del p.(Asp2284del) *De novo*	Infantile EE with IS evolving to myoclonic seizures	8 m	At 14 m ETP in sleep during spasms, no hypsarrhythmia, at 22 m no ETP increased beta activity	IS evolving into myoclonic seizures, seizure free after 15 m	LEV	Severe DD, hypotonia, ataxic movement disorder; No specific dysmorphic features	Pontocerebellar hypoplasia/ atrophy; subependymal heterotopia, thin CC, at 12 m (Supplementary Fig. 2)	47.3 cm (−1.2), at 2 y	Novel
10/F	3 y 6 m[a]	c.6908_6916dup p.(Asp2303_2305dup) *De novo*	West syndrome	2 m	Hypsarrhythmia, at 3 y background slowing and multifocal ETP	Ongoing spasms and TS until death	LEV + PB (ACTH partially effective on IS, TPM, Pred, KD)	Profound DD, hypotonia, ataxia, dyskinetic movement disorder, lack of visual attention; Microcephaly, thick dorsum of hands and feet	Global atrophy, more pronounced on cerebellum / brainstem, thin CC, hypomyelination, at 2 y 5 m (Fig. 2)	32.5 cm (−1.78) / 42 cm (−7.62), at 3 y	Nonoda *et al.*, 2013; Tohyama *et al.*, 2015
11/M	6 y	c.6908_6916dup p.(Asp2303_2305dup) *De novo*	West syndrome (PEHO)	4 m	Hypsarrhythmia	Persisting focal and reflex seizures	n.a.	Profound DD, hypotonia, lack of visual attention; Microcephaly, thick dorsum of hands and feet	Global brain, brainstem and cerebellar atrophy, thin CC, hypomyelination, at 4 y 7 m (Fig. 2)	33 cm (−1.28) / 45 cm (−5.4), at 6 y	Nonoda *et al.*, 2013; Tohyama *et al.*, 2015

(continued)

Table 1 Continued

Patient/ gender	Age at last follow-up	Mutation	Epilepsy syndrome	Seizure onset	EEG	Seizure outcome	Current treatment (previous medication)	Development; Clinical examination	Brain MRI	OFC at birth/postnatal OFC at last follow-up (SD score)	Reference
12/F	2 y	c.6908_6916dup p.(Asp2303_2305dup) *De novo*	Infantile frontal lobe seizures evolving to West syndrome	5 m	Hypsarrhythmia at 14 m, at 2 y diffuse low amplitude activity without ETP	Cessation of spasms at 14 m, ongoing FDS, frontal lobe seizures	VPA + ZNS (PLP, LEV not effective; ACTH effective for spasms)	Profound DD, hypotonia, lack of visual attention; Microcephaly	Global atrophy, more pronounced on cerebellum/ brainstem, thin CC, hypomyelination, at 1 y 9 m (Supplementary Fig. 2)	32 cm (−0.6) / 36.9 cm (−3.14), at 5 m	Nonoda *et al.*, 2013; Tohyama *et al.*, 2015
13/M	5 y 7 m[a]	c.6907_6915dup p.(Asp2303_2305dup) *De novo*	West syndrome	4 m	Hypsarrhythmia, persisting at 2 y	Ongoing spasms until death	LEV (VGB, TPM)	Profound DD, multifocal myoclonus, dyskinetic movement disorder, intermittent opisthotonus, hypotonia, lack of visual attention; Microcephaly	Cerebellar vermis hypoplasia/thin CC, hypomyelination, at 3 m (Supplementary Fig. 2)	31.5 cm (−3) / 42 cm (−8), at 5 y	Nonoda *et al.*, 2013; Tohyama *et al.*, 2015
14/F	4 y 3 m[a]	c.6907_6915dup p.(Asp2303_2305dup) *De novo*	West syndrome	4 m	Hypsarrhythmia at 4 m, at 3 y Multifocal discharges and slowing, no hypsarrhythmia	Cessation of IS at 7 m, later tonic seizures	VPA (VGB, Pred, B6, TPM)	Profound DD, intermittent opisthotonus, hypotonia, lack of visual attention Microcephaly	Global brain, brainstem / cerebellar atrophy, thin CC, hypomyelination, at 2 y 2 m (Supplementary Fig. 2)	31.5 cm (−2.5) / 42 cm (−7), at 3.5 y	Nonoda *et al.*, 2013; Tohyama *et al.*, 2015
16/M	6 y	c.6910_6918del p.(Gln2304_Gly2306del) *De novo*	West syndrome	4 m	Hypsarrhythmia, at 5 y normal EEG	Seizure free after ACTH at 7 m	VPA (PLP with partial effectiveness, ACTH effective for IS)	Mild ID, DD, Delayed walking (26 m), mild attention deficit; Depressed nasal bridge, frontal bossing	Mild ventricular dilatation, thin CC, at 5 m (Supplementary Fig. 2)	34 cm (+0.96) / 52.7 cm (+0.67), at 6 y	Novel, but duplication c.6910_6918dup associated with West syndrome
17/M	3 y	c.6923_6928dup p.(Arg2308_Met2309dup) *De novo*	West syndrome	3 m	Hypsarrhythmia	Persisting spasms, TS, myoclonic seizures	VGB + TPM + LEV (PB, VPA, ESM)	Profound DD, lack of visual attention; Microcephaly	Global atrophy, more pronounced on cerebellum/ brainstem, thin CC, hypomyelination, at 3 y 6 m (Fig. 2)	32 cm (−2.08) / 44 cm (−4), at 3 y	Saitsu *et al.*, 2010
Individuals with *de novo* variants in *SPTAN1* and childhood onset epilepsy syndromes											
1/M	4 y 6 m	c.533G>A p.(Gly178Asp) *De novo*	Focal	3 y	Bilateral frontal spikes	Seizure-free on PB	PB	Normal; Normal	Normal at 3 y (Supplementary Fig. 3)	37 cm (+0.67) / 50 cm (0), at 3 y	Novel
2/M	18 y	c.917C>T p.(Ala306Val) *De novo*	Epilepsy with myoclonic and atonic seizures	2 y 2 m	Normal at 2 y, multifocal discharges at 6 y and 16 y	Seizure-free on VPA, 1 y seizure free with no medication, till seizures relapse at 5 y	VPA	Moderate ID, able to walk; Normal	Normal at 7 y 3 m (Supplementary Fig. 3)	39.5 cm (+2.2) / 60 cm (+2), at 18 y	Novel
3/M	10 y	c.3716A>G p.(His1239Arg) *De novo*	No epilepsy	NA	n.a.	NA	NA	Mild DD, ID, ASD; Mild dysmorphic signs, no microcephaly	n.a.	n.a. (normal OFC)	Novel
4/M	10 y	c.4828C>T p.(Arg1610Trp) *De novo*	Myoclonic epilepsy	2 y	Persisting generalized SW, poly-SW	Febrile seizures	VPA (LEV, LTG)	Mild–moderate DD, ID, ASD, hypotonia, walks with mild spasticity; Increased tone and deep tendon reflexes in lower limbs, autistic behaviour	Cerebellar atrophy, cervical syringomyelia, at 8 y (Fig. 2)	n.a. / 53 cm (+0.33), at 7 y	Novel

(continued)

Table 1 Continued

Patient/ gender	Age at last follow-up	Mutation	Epilepsy syndrome	Seizure onset	EEG	Seizure outcome	Current treatment (previous medication)	Development; Clinical examination	Brain MRI	OFC at birth/postnatal OFC at last follow-up (SD score)	Reference
15/M	19 y	c.6908_6916del p.(Asp2303_Leu2305del) *De novo*	FDS	At 17 m febrile seizures, since 5 y focal seizures	Focal spikes	Seizure-free on PB	PB (VPA)	Moderate ID, ADHD; Normal	Normal at 16 y (Supplementary Fig. 3)	36 cm (0) / 59 cm (+ 1.3), at 19 y	Novel
18/F	16 y	arr[hg19] 9q34.11 (131,349,701–131,351,531)x1 exon 20–21 deletion p.(Ala927_Lys1002del) *De novo*	Focal seizures (left arm and head shaking)	15 y	Normal	No further seizures	None	Mild DD, ID, mild diffuse hypotonia, slowly progressive and severe cerebellar ataxia; Wheelchair bound	Severe cerebellar atrophy, at 13 y 9 m and 15 y 7 m (Fig. 2)	n.a. / 56 cm (+ 0.67), at 16 y	Novel

ASD = autism spectrum disorder; ACTH = adrenocorticotropic hormone; ADHD = attention deficit hyperactivity disorder; B6 = pyridoxine; CBZ = carbamazepine; CC = corpus callosum; CLB = clobazam; CZB = clonazepam; DD = developmental delay; EE = epileptic encephalopathy; ESM = ethosuximide; ETP = epileptiform potentials; F = female; FDS = focal dyscognitive seizures; ID = intellectual disability; IS = infantile/epileptic spasms; KD = ketogenic diet; LEV = levetiracetam; LTG = lamotrigine; m = months; M = male; NA = not applicable; n.a. = not available; OFC = occipitofrontal head circumference (microcephaly was defined as OFC <2 SD score according to country-specific control cohorts; WHO child growth standards and the Fenton growth chart for preterm infants); PB = phenobarbital; PEHO = progressive encephalopathy with oedema; hypsarrhythmia and optic atrophy; poly-SW = poly spike and wave discharge; PLP = pyridoxal 5'-phosphate; Pred = prednisone; STM = sultiame; SW = spike and wave discharges; TPM = topiramate; TS = tonic seizures; VGB = vigabatrin; VPA = valproic acid; y = years; ZNS = zonisamide.
[a]Deceased.

exhibiting oedema of hands and feet in the context of West syndrome and blindness (Table 1).

Microcephaly was present in 11/14 (79%) patients with epileptic encephalopathy and was significantly associated with a poor developmental outcome in our cohort ($P < 0.05$, U-test). When primary microcephaly was noted at birth (3/14, 21%), it was associated with EIEE5.

Six patients (6/20, 30%) did not present with early infantile epileptic encephalopathy and were classified as a group with childhood-onset epilepsy syndromes (Table 1). In five patients (5/6, 83%; 25% of all), different epilepsy syndromes were diagnosed comprising focal (3/5, 60%) or myoclonic epilepsy (2/5, 40%), with an onset ranging from 2–15 years of age. One patient (Patient 3) did not develop epilepsy until 10 years of age (Table 1). Seizure outcome was favourable in this group as seizures were controlled with one single AED or even without pharmacotherapy (Patient 18). Five of six patients in this group exhibited mild to moderate developmental delay and intellectual disability (5/6, 83%) (Table 1).

Neuroimaging data

Brain MRI was available in 19 individuals and showed structural abnormalities in 15 (15/19, 79%; 13/14, 93% of those with epileptic encephalopathy). In all nine individuals who underwent repeated MRI, there was worsening of circumscribed and generalized cerebral atrophy and delayed myelination (Fig. 2 and Supplementary Fig. 1). Overall, we confirmed a variable degree of atrophy affecting cortex, brainstem and/or cerebellum (13/14, 93% with epileptic encephalopathy; 15/19, 79% overall), hypomyelination (11/14, 79% with epileptic encephalopathy, 11/19, 58% overall), and thinning of the corpus callosum (12/14, 86% with epileptic encephalopathy; 12/19, 63% overall) to be the main MRI abnormalities in *SPTAN1* encephalopathy. One individual had cervical syringomyelia (Patient 4) (1/20, 5%), one had mild ventricular dilatation (Patient 16), and one an isolated nodule of periventricular heterotopia (Patient 20) (1/20, 5%).

In more detail, 6 of 15 patients showing an abnormal MRI were imaged only once when aged 3 months to 2 years 2 months (Patients 7, 12–14, 16 and 20; Supplementary Fig. 2). They exhibited various combinations of the aforementioned structural abnormalities, which were much more severe in Patients 12 and 14, imaged at an older age (>1 year 9 months) with respect to the remaining four (Patients 7, 13, 16 and 20) who were imaged when aged 3 to 12 months. Nine patients underwent repeated imaging after the first MRI at ages of 2 months to 3 years 3 months, which revealed some degree of abnormality (Patients 4–6, 8–11, 17 and 18; Fig. 2 and Supplementary Fig. 1). The second MRI at ages 6 months to 14 years showed progressive atrophic changes in all, leading to isolated cerebellar atrophy in two patients with childhood-onset epilepsy (Patients 4 and 18) and to a generalized atrophy of brain, brainstem and cerebellum in the remaining individuals

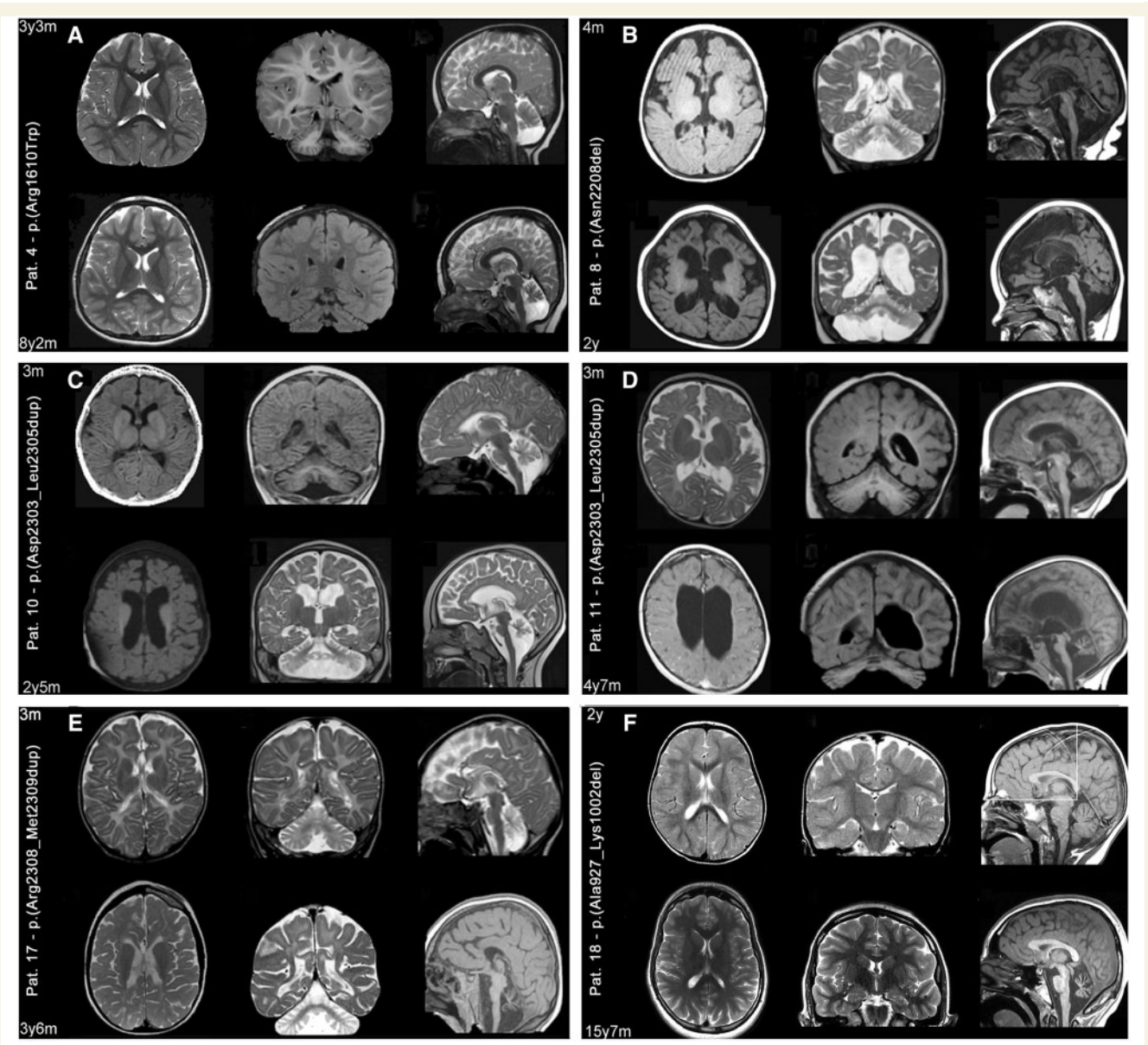

Figure 2 Progression of structural MRI abnormalities. Six representative patients [Patients 4 (**A**), 8 (**B**), 10 (**C**), 11 (**D**), 17 (**E**) and 18 (**F**)] are shown of the nine patients with *SPTAN1* variants who were imaged at least twice during follow-up (comparative follow-up images for Patients 5, 6 and 9 are presented in Supplementary Fig. 1). For each patient (**A–F**) two sets of comparative axial (*left column*), coronal (*middle column*) and sagittal (*right column*) images are presented, taken respectively from the initial and follow-up investigations. Images are at 1.5 to 3 T and include T_1-weighted, T_2-weighted and fluid-attenuated inversion recovery (FLAIR) sequences. Structural abnormalities include a combination of cerebellar and brainstem atrophy, dilated ventricles and subarachnoid spaces, thinning of the corpus callosum and hypomyelination that are variably distributed. Here, however, comparison of initial and follow-up images demonstrates different rates of progression from one patient to another and from one involved structure to another. For example, in Patient 4 (**A**), who harbours a missense variant falling outside the heterodimerization domain, from age 3 years 3 months to age 8 years 2 months, only cerebellar atrophy has really worsened; and in Patient 18 (**F**), who harbours an in-frame deletion also falling outside the heterodimerization domain, MRI scan at age 2 years was still normal but exhibited isolated, severe cerebellar atrophy at age 15 years. In all remaining patients, harbouring different types of mutations falling within the heterodimerization domain, follow-up images demonstrate severely progressive changes that are generalized, involving the brain, cerebellum and brainstem, although not uniformly, and more prominent in patients imaged at older ages (see for example Patients 8, 10, 11 and 17).

with infantile epileptic encephalopathy (Patients 5, 6, 8–11 and 17). However, the rate of progression was variable showing only mild worsening over long periods in some patients. For example, cerebellar atrophy progressed only mildly in Patient 4 from age 3 years 3 months to 8 years 2 months (Fig. 2). In contrast, other patients demonstrated severe worsening of atrophy within only 2–3 years (Patients 8–11 and 17; Fig. 2).

Hypomyelination was observed in 11 patients with early infantile epileptic encephalopathy (Patients 5–14 and 17)

and was always associated with atrophic changes (Fig. 2, Supplementary Fig. 1 and 2).

The five patients (5/20; 1/14 of those with infantile epileptic encephalopathy) with normal MRI (Patients 1–3, 15 and 19; Supplementary Fig. 3) were studied between 2 years 10 months and 16 years, corresponding to an age range within which atrophic changes were already obvious in all other patients.

Mutational spectrum

In our cohort of 20 individuals, we identified 16 different *SPTAN1* sequence alterations, 12 of which were novel (Fig. 1 and Supplementary Table 2). The seven observed missense variants were predicted to alter evolutionarily highly conserved residues and were located in spectrin repeats α2, α3, α11, α14, α16, α18 and α20 (Fig. 1).

Nine different in-frame deletions and duplications, of which eight affected the heterodimerization domain (spectrin repeats α19 and α20), included the known mutations p.(Glu2207del), c.6908_6916dup and c.6907_6915dup, both predicting p.(Asp2303_Leu2305dup), and p.(Arg2308_2309dup). Novel mutations were p.(Asn2208del), p.(Asp2284del), p.(Asp2303_Leu2305del) and p.(Gln2304_Gly2306del). With p.(Ala927_Lys1002del), we report the first in-frame deletion affecting the SH3 domain within repeat α9 in a patient with childhood-onset epilepsy and ataxia (Patient 18), defined as slowly progressive spinocerebellar ataxia (Table 1).

Recurrent variants included p.(Asp2303_Leu2305dup) in 5/20 patients and p.(Glu2207del) in 2/20. None of the 16 different *SPTAN1* variants are listed in the ExAC browser (http://exac.broadinstitute.org/). Pathogenicity of variants was classified according to ACMG guidelines (Supplementary Table 2).

The two in-frame deletions p.(Asp2303_Leu2305del) and p.(Gln2304_Gly2306del) in Patients 15 and 16 are located in the αII spectrin repeat α20, at positions where duplications have previously been reported in patients with EIEE5 and profound intellectual disability (Nonoda *et al.*, 2013; Ream and Mikati, 2014).

Functional consequences of *SPTAN1* mutations in patient-derived fibroblasts

We used fibroblasts of five patients with p.(Ala306Val), p.(Glu2207del), p.(Asp2303_Leu2305dup), p.(Asp2303_Leu2305del), and p.(Arg2308_Met2309dup) as a model system to examine the effects of different *SPTAN1* variants (Fig. 1). Immunostaining of αII and βII spectrins revealed a more or less even distribution of the two proteins throughout fibroblasts of a control person (Fig. 3A), which is in line with the location of the spectrin-based skeleton at the inner surface of the plasma membrane (Machnicka *et al.*, 2014). In fibroblasts of Patients 10 and 17 with p.(Asp2303_Leu2305dup) and p.(Arg2308_Met2309dup), we observed aggregations of αII spectrin in all cells examined. These aggregates co-localized with βII spectrin and predominantly clustered near or at the plasma membrane (Fig. 3A). αII/βII spectrin aggregates were also observed in fibroblasts from the patient with p.(Glu2207del); however, the aggregates had a lower immunofluorescence brightness compared to those in cells of Patients 10 and 17 (Fig. 3A). No spectrin aggregation was detected in fibroblasts of the patients with p.(Ala306Val) and p.(Asp2303_Leu2305del) variants (Patients 2 and 15; Fig. 3A).

Aggregation of αII/βII spectrin heterodimers in three patient-derived fibroblasts prompted us to prepare Triton™ X-100 soluble and insoluble protein fractions from fibroblast cells of the five patients and three controls. Upon aggregation of αII and βII spectrins, aggregates are expected to be present in the insoluble protein fraction. In control cells and cells derived from patients with *SPTAN1* variants p.(Ala306Val) and p.(Asp2303_Leu2305del), αII spectrin was mainly present in the soluble fraction (Fig. 3B). Similarly, αII spectrin still was associated with the soluble protein fraction in fibroblasts of Patients 6 [p.(Glu2207del)], 10 [p.(Asp2303_Leu2305dup)], and 17 [p.(Arg2308_Met2309dup)]; however, it was clearly enriched in the insoluble protein fraction in these three fibroblast cell lines (Fig. 3B). Altogether, the data confirmed the presence of spectrin aggregates in fibroblasts of Patients 6, 10 and 17.

We hypothesized that patient-derived fibroblasts with αII/βII spectrin aggregates may be more vulnerable to apoptosis and/or show enhanced cleavage of αII spectrin. Therefore, we treated two control fibroblast cell lines and patient-derived fibroblasts with visible αII/βII spectrin aggregates (Patients 10 and 17) with staurosporine for 0, 4, 8, 24 and 48 h to induce apoptosis and detected full-length and cleaved αII spectrin by immunoblotting. We observed no differences in the amount of cleaved αII spectrin between control and patients' fibroblasts at different time points (Supplementary Fig. 4A). Similarly, we found no difference in BrdU-positive cells upon staurosporine-induced apoptosis between the two patient-derived fibroblasts cells with *SPTAN1* variants p.(Asp2303_Leu2305dup) and p.(Arg2308_Met2309dup) and control cells (Supplementary Fig. 4B). We induced autophagy by culturing fibroblasts of Patients 10 and 17 and two control individuals in starvation medium and observed the same amount of the autophagy marker LC3-II in all cells (Supplementary Fig. 5A). In line with this finding, the amount of beclin 1, another autophagy marker, was similar in patients' and control fibroblasts (Supplementary Fig. 5B).

Molecular modelling of *SPTAN1* missense variants

To gain first insight into the consequences of the *SPTAN1* missense variants identified here, we explored the structural impact of the variants by a homology model for two

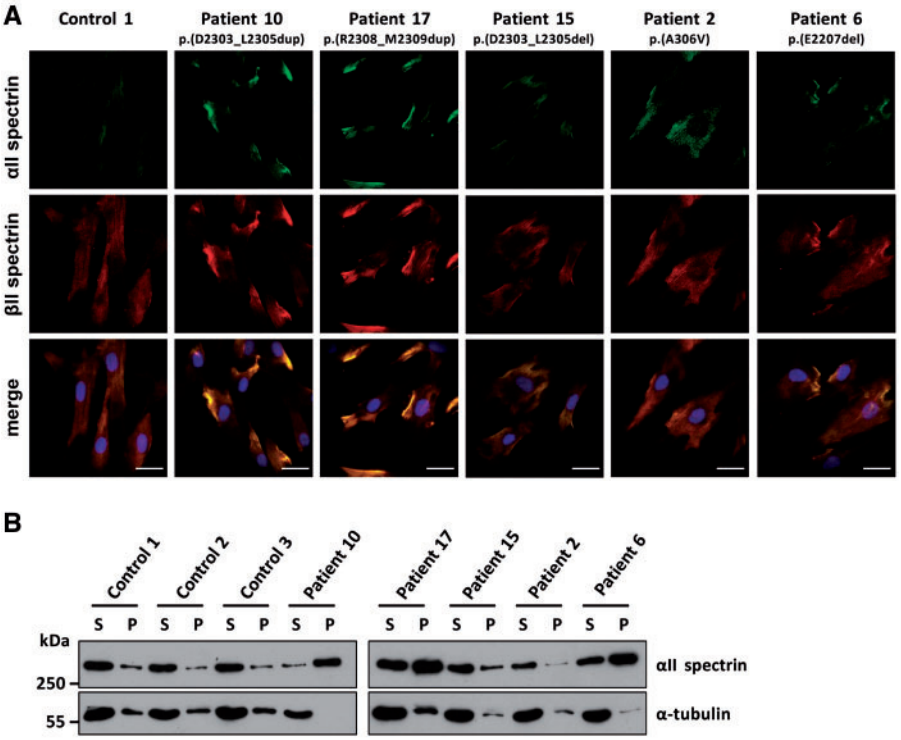

Figure 3 Spectrin aggregate formation in fibroblast cells of three patients with an in-frame deletion/duplication in *SPTAN1*. (**A**) Primary fibroblasts of Patients 2, 6, 10, 15 and 17 and a control individual were co-stained by mouse anti-αII spectrin and rabbit anti-βII spectrin antibodies followed by anti-mouse Alexa Fluor® 488 (green) and anti-rabbit Alexa Fluor® 546 (red) conjugated secondary antibodies, respectively, and embedded in mounting solution with DAPI (blue). Camera settings were the same for all images shown, and images were not further processed (see 'Material and methods' section). Representative images are shown. Scale bars = 20 μm. (**B**) Fibroblast cells of Patients 2, 6, 10, 15, and 17 and three control individuals were subjected to Triton™ X extraction. Supernatant (S) and pellet (P) were analysed by SDS-PAGE and immunodetection using antibodies against αII spectrin and α-tubulin as a control. Representative blots of three independent experiments are shown.

spectrin repeats (Supplementary Fig. 6). For four of the seven amino acid substitutions, this analysis predicted steric clashes and/or disruption of salt bridges between helices of the spectrin repeats (Supplementary Fig. 6), suggesting that the amino acid changes induce larger structural alterations and possible conformational changes in αII spectrin.

Discussion

We present the currently largest series of patients with pathogenic or likely pathogenic *SPTAN1* variants and define the phenotypic spectrum of *SPTAN1*-related disorders. Including previously published observations, 34 individuals harbouring 22 different *SPTAN1* variants are now known (Supplementary Tables 1 and 2), comprising 11 missense variants, 10 in-frame deletions/duplications, and one truncating variant (Supplementary Tables 1 and 2).

Genotype–phenotype correlations

In line with the known *SPTAN1*-associated clinical features (Saitsu *et al.*, 2010; Hamdan *et al.*, 2012; Writzl *et al.*, 2012; Nonoda *et al.*, 2013; Ream and Mikati, 2014; Tohyama *et al.*, 2015), we found *SPTAN1* encephalopathy to be associated with seizures (95% of our patients, 85%, including published cases), most frequently presenting as infantile-onset epileptic encephalopathy in 62% of affected children (14/20 in this report, 21/34, including published cases). Apart from one patient with predominant tonic seizures, all individuals with infantile epileptic encephalopathy presented with infantile spasms (20/34, 59%) (Table 1 and Supplementary Table 1). This group of patients (21/34, 62%) with a severe form of an early onset epileptic encephalopathy represents the severe end of the clinical spectrum associated with *de novo SPTAN1* variants.

The most severe form of *SPTAN1* encephalopathy has been delineated as EIEE5 (Saitsu *et al.*, 2010) and was present in 50% of all reported patients (7/14 published cases and 10/20 in this report) (Table 1 and Supplementary Table 1). Patients with EIEE5 in our study presented with West syndrome, and EEG constantly showed hypsarrhythmia, persisting over a long time (up to 3 years in single cases) or evolving to disorganized slow background activity in all with multifocal spikes in most (90%). Treatment of seizures with AED was challenging and infantile spasms remained refractory in the vast majority of cases with

infantile onset epileptic encephalopathy. Only in two of our patients, infantile spasms responded to the first AED (Patients 16 and 19), while they proved refractory to medication in all remaining patients (Table 1), likewise previously reported (Tohyama *et al.*, 2015). We also found that the severe spectrum of *SPTAN1* encephalopathy is associated with milder forms of infantile epileptic encephalopathy (4/14, 29%), partially lacking specific EEG or brain imaging features.

Brain imaging in the group of patients with infantile epileptic encephalopathy revealed significant worsening of generalized and pontocerebellar atrophy with delayed and incomplete myelination. In general, the spectrum of MRI findings in *SPTAN1* encephalopathy shows similarities to early stages of Pelizaeus-Merzbacher disease with respect to white matter changes (Supplementary Fig. 7A–C) as well as to pontocerebellar hypoplasia type 2, which may feature similar hypoplastic cerebellar and brainstem changes (Supplementary Fig. 7D–F).

Patients with EIEE5 experienced developmental arrest after onset of infantile spasms and never achieved gross motor and communicative skills, nor did they acquire visual attention. Primary microcephaly was only present in patients with the diagnosis of EIEE5.

SPTAN1 encephalopathy may manifest with oedematous extremities and blindness (Tohyama *et al.*, 2015), which led to the initial diagnosis of PEHO syndrome in one of our patients (1/20; 5%). Ocular manifestations, such as coloboma-like optic discs were present in only 1/14 (7%) previously reported patients (Writzl *et al.*, 2012). Although poor visual attention is a common feature in *SPTAN1* encephalopathy, optic atrophy at fundoscopy remained rare.

The premature death of four patients in our cohort and three of those previously reported (7/34, 21%) suggests a high prevalence of early childhood death in patients with *SPTAN1* encephalopathy (this study, Saitsu *et al.*, 2010 and personal communication; Nonoda *et al.*, 2013). Recently, another *de novo SPTAN1* variant was reported as a candidate pathogenic variant for SUDEP (Bagnall *et al.*, 2016).

All patients with infantile epileptic encephalopathy carried amino acid changes and in-frame deletions/duplications between positions Arg1776 and Met2309 (6/8 in our study, 9/11 overall) located in the αII spectrin repeats α16 to α20. The two Patients 5 and 19 with mutations in α16 and α18 exhibited some distinctive features. Patient 19 acquired normal developmental skills and had a normal brain MRI despite having had West syndrome and Patient 5 was diagnosed with an unspecific epileptic encephalopathy with tonic and focal seizures. All individuals with the most severe form of EIEE5 (10/20 in our group, 17/34 overall) carried mutations in αII spectrin repeat α19 and α20 with p.(Asp2303_Leu2305dup) being the single most recurrent variant (5/20 in our group, 8/34 in all). Additional recurrent variants were p.(Glu2207del) in 4/34 (2/20 in our group), and p.(Arg2308_Met2309dup) in 2/34 (1/20 in our group).

In contrast to the patient group with infantile epileptic encephalopathy, 30% of our patients (6/20) had less severe intellectual disability and milder forms of epilepsy with childhood onset, such as generalized, myoclonic, focal, or even no epilepsy. The relatively mild phenotype of this patient cohort lies at the other end of the spectrum of *SPTAN1*-related disorders. In these patients, epileptic seizures started after infancy, and seizures were less disabling and associated with a favourable response to AEDs.

Brain imaging in these individuals was normal (3/5, 60%) or showed only partial overlap to the more severely affected with milder progressive cerebellar atrophy (2/5, 40%) being the main feature. These individuals were more likely to carry missense variants (4/6, 67%) and variants lying outside the heterodimerization domain (5/6, 83%) (Table 1). *De novo* variants outside the C-terminal repeats α16 to α20 were mainly found in individuals with normal cognition or mild to moderate intellectual disability and ataxia similar to the two reported individuals with the *SPTAN1 de novo* variants p.(Glu91Lys) (Gilissen *et al.*, 2014) and p.(Arg566Pro) (Hamdan *et al.*, 2012).

One individual with childhood onset epilepsy and normal MRI [Patient 15 with p.(Asp2303_Leu2305del)] and one with West syndrome and mild MRI abnormalities [Patient 16 with p.(Gln2304_Gly2306del)] carried in-frame deletions within repeat α20, at positions where duplications have previously been associated with EIEE5 and profound intellectual disability (Nonoda *et al.*, 2013; Ream and Mikati, 2014). In contrast to single amino acid deletions (p.Glu2207del, p.Asn2208del and p.Asp2284del), the two aforementioned larger in-frame deletions in spectrin repeat α20 as well as p.(Ala927_Lys1002del) in α9 were associated with mild to moderate intellectual disability and seizures that responded relatively well to antiepileptic medication (Patients 15 and 16), or did not require treatment at all (Patient 18). Of note, Patient 18 with a distinct variant in the SH3 domain within repeat α9 [p.(Ala927_Lys1002del)] had a unique phenotype consisting of mild intellectual disability, normal head circumference and slowly progressive spinocerebellar ataxia and isolated cerebellar atrophy with only a few unconfirmed seizures not requiring treatment.

Functional consequences of *SPTAN1* variants

In fibroblasts of three patients (Patients 6, 10, and 17) with the amino acid alterations p.(Glu2207del), p.(Asp2303_Leu2305dup) and p.(Arg2308_Met2309dup), we identified protein aggregates of αII/βII spectrin heterodimers that are reminiscent of αII/βII and αII/βIII spectrin aggregates in lymphoblastoid cells of patients with p.(Glu2207del) and p.(Arg2308_Met2309dup) and aggregates found in cultured cortical neurons ectopically expressing either of the two aforementioned αII spectrin mutants (Saitsu *et al.*, 2010). We also detected αII spectrin in the insoluble protein

fraction in fibroblasts of patients with p.(Glu2207del), p.(Asp2303_Leu2305dup) and p.(Arg2308_Met2309dup), providing additional evidence for its aggregation. This finding might indicate that αII spectrin loosens its interaction with the membrane, thereby disturbing the membrane skeletal network in fibroblast cells.

The two variants p.(Asp2303_Leu2305dup) and p.(Arg2308_Met2309dup) analysed here as well as p.(Gln2304_Gly2306dup) are consistently associated with the most severe neurological phenotype of EEIE5 (Saitsu *et al.*, 2010; Nonoda *et al.*, 2013; Ream and Mikati, 2014; Tohyama *et al.*, 2015). These in-frame duplications repeatedly affect the amino acid stretch 2303-Asp-Gln-Leu-Gly-Met-Arg-Met-2309, located in the last αII spectrin repeat 20 required for heterodimer formation (Ursitti *et al.*, 1996; An *et al.*, 2011). Initiation of spectrin dimerization is dependent on complementary long range electrostatic interactions between α19-α20 and β1-β2 repeats of α and β spectrin monomers, respectively (Begg *et al.*, 2000). Duplication of two to three amino acid residues within this amino acid stretch could either disrupt the tertiary structure of α20, a triple-helical bundle, or alter the charge of this amino acid stretch leading to changes in electrostatic interactions during the dimer initiation process. Duplications within this seven-amino acid stretch seem to have a more severe effect on α/β heterodimerization than deletions, such as the p.(Asp2303_Leu2305del) variant, as no aggregates have been detected in fibroblasts of the respective patient. These findings suggest that the amino acid stretch 2303-Asp-Gln-Leu-Gly-Met-Arg-Met-2309 is highly important for α/β heterodimerization and/or spectrin function in the brain, and amino acid duplications that fall within this region have more severe consequences on spectrin dimer formation than deletions.

In fibroblasts of Patient 2 with the missense variant p.(Ala306Val), αII/βII heterodimer aggregates were not observed by immunocytochemistry. Molecular modelling of the seven missense variants identified here provide preliminary evidence for structural alterations of the A-, B- and/or C-helices within the mutated spectrin repeats. However, further experiments are required to show if these amino acid changes and other in-frame variants in *SPTAN1* alter αII spectrin's structural and mechanical properties and/or interactions with cytoskeletal, signal transduction and membrane integral proteins (Machnicka *et al.*, 2014).

By using patient-derived fibroblast cells as model system, we obtained no evidence for increased apoptosis or impaired autophagy due to *SPTAN1* variants, not even in cells derived from severely affected patients with p.(Asp2303_Leu2305dup) or p.(Arg2308_Met2309dup). However, neuronal cells may be more vulnerable to spectrin aggregate formation and/or any other disturbances in αII spectrin function, leading to severe functional disruption in the nervous system. Indeed, αII spectrin has been demonstrated to be essential for the axonal cytoskeleton: it stabilizes nascent sodium-channel clusters and assembles the node of Ranvier (Voas *et al.*, 2007), and αII spectrin together with ankyrinB and βII spectrin controls the length and position of the axon initial segment (Galiano *et al.*, 2012). In Schwann cells, αII and βII spectrins function as key regulators of myelination (Susuki *et al.*, 2011). Collectively, these data suggest that dysregulation or disruption of the spectrin-based submembranous cytoskeleton in various cell types of the nervous system might contribute to the broad neurological spectrum of patients with *SPTAN1* mutations. Our results, together with previous reports, show that distinct alterations at specific locations are less tolerated than haploinsufficiency of *SPTAN1* (Saitsu *et al.*, 2010; Campbell *et al.*, 2012; Tzschach *et al.*, 2012; Tohyama *et al.*, 2015), which might open windows for future gene targeted treatments in the severely affected patients who are refractory to current therapies.

Conclusion

Our study provides evidence for a role of *SPTAN1* mutations in a wide spectrum of developmental encephalopathies. Infantile onset of different epileptic encephalopathy together with progressive atrophy of the cerebellum and brainstem is the hallmark in patients with a severe form of *SPTAN1* encephalopathy. Patients with *SPTAN1* encephalopathy have a relevant risk for premature and unexpected death. In addition, we broadened the phenotypic spectrum of *SPTAN1*-related disorders by defining a group of patients with less severe intellectual disability, different types of childhood onset epilepsy and without any sign of progression. The pathobiology is likely driven by aggregation and failure of heterodimerization of α and β spectrins in patients exhibiting severe infantile epileptic encephalopathy with a neurodegenerative character. The pathophysiology underlying the milder phenotypes might be related to more subtle changes of neuronal excitability and mechanisms other than spectrin aggregation. Further studies will be helpful to shed light on the role of *SPTAN1* in these static neurological developmental disorders.

Acknowledgements

We thank all patients and family members for their participation in this study, Malik Alawi for bioinformatics analysis of whole-exome sequencing data of Patient 10, Hans-Jürgen Kreienkamp for help with structural analysis and critical reading, and the Microscopy Imaging Facility (UMIF) at the University Medical Center Hamburg-Eppendorf for technical support. We kindly acknowledge all involved clinicians and radiologists for providing clinical and MRI data.

Funding

This work was supported by a grant of the Deutsche Forschungsgemeinschaft (KU 1240/10-1 to K.K.); the EU

7th Framework Programme (FP7) under the project DESIRE grant N602531 (to R.G.); a grant from the Dietmar-Hopp-Stiftung (23011236 to S.S.), Practical Research Project for Rare/Intractable Diseases (27280301 to M.K. and 26310501 to N.M.) from Japan Agency for Medical Research and development, AMED; and the Federal Ministry of Education and Research (BMBF), Germany (FKZ: 01EO1501 to H.O.H.).

Conflict of interest

K.L.H. is employed by Ambry Genetics, a company that provides *SPTAN1* sequencing in the setting of gene panel testing and whole-exome sequencing among its commercially available tests. S.B. is working for CeGaT Gmbh, a company that provides *SPTAN1* sequencing in the setting of gene panel testing and whole-exome sequencing among its commercially available tests.

Supplementary material

Supplementary material is available at *Brain* online.

References

An JY, Cristino AS, Zhao Q, Edson J, Williams SM, Ravine D, et al. Towards a molecular characterization of autism spectrum disorders: an exome sequencing and systems approach. Transl Psychiatry 2014; 4: e394.

An XL, Guo XH, Yang Y, Gratzer WB, Baines AJ, Mohandas N. Inter-subunit interactions in erythroid and non-erythroid spectrins. Biochim Biophys Acta 2011; 1814: 420–7.

Bagnall RD, Crompton DE, Petrovski S, Lam L, Cutmore C, Garry SI, et al. Exome-based analysis of cardiac arrhythmia, respiratory control, and epilepsy genes in sudden unexpected death in epilepsy. Ann Neurol 2016; 79: 522–34.

Begg GE, Harper SL, Morris MB, Speicher DW. Initiation of spectrin dimerization involves complementary electrostatic interactions between paired triple-helical bundles. J Biol Chem 2000; 275: 3279–87.

Campbell IM, Yatsenko SA, Hixson P, Reimschisel T, Thomas M, Wilson W, et al. Novel 9q34.11 gene deletions encompassing combinations of four Mendelian disease genes: STXBP1, SPTAN1, ENG, and TOR1A. Genet Med 2012; 14: 868–76.

Cellini E, Vignoli A, Pisano T, Falchi M, Molinaro A, Accorsi P, et al. The hyperkinetic movement disorder of FOXG1-related epileptic-dyskinetic encephalopathy. Dev Med Child Neurol 2016; 58: 93–7.

Czogalla A, Sikorski AF. Spectrin and calpain: a 'target' and a 'sniper' in the pathology of neuronal cells. Cell Mol Life Sci 2005; 62: 1913–24.

de Kovel CG, Brilstra EH, van Kempen MJ, van't Slot R, Nijman IJ, Afawi Z, et al. Targeted sequencing of 351 candidate genes for epileptic encephalopathy in a large cohort of patients. Mol Genet Genomic Med 2016; 4: 568–80.

Dubielecka PM, Grzybek M, Kolondra A, Jazwiec B, Draga A, Aleksandrowicz P, et al. Aggregation of spectrin and PKC theta is an early hallmark of fludarabine/mitoxantrone/dexamethasone-induced apoptosis in Jurkat T and HL60 cells. Mol Cell Biochem 2010; 339: 63–77.

Galiano MR, Jha S, Ho TS, Zhang CS, Ogawa Y, Chang KJ, et al. A Distal axonal cytoskeleton forms an intra-axonal boundary that controls axon initial segment assembly. Cell 2012; 149: 1125–39.

Gilissen C, Hehir-Kwa JY, Thung DT, van de Vorst M, van Bon BW, Willemsen MH, et al. Genome sequencing identifies major causes of severe intellectual disability. Nature 2014; 511: 344–7.

Hamdan FF, Saitsu H, Nishiyama K, Gauthier J, Dobrzeniecka S, Spiegelman D, et al. Identification of a novel in-frame *de novo* mutation in SPTAN1 in intellectual disability and pontocerebellar atrophy. Eur J Hum Genet 2012; 20: 796–800.

Helbig KL, Farwell Hagman KD, Shinde DN, Mroske C, Powis Z, Li S, et al. Diagnostic exome sequencing provides a molecular diagnosis for a significant proportion of patients with epilepsy. Genet Med 2016; 18: 898–905.

Higasa K, Miyake N, Yoshimura J, Okamura K, Niihori T, Saitsu H, et al. Human genetic variation database, a reference database of genetic variations in the Japanese population. J Hum Genet 2016; 61: 547–53.

Kortum F, Caputo V, Bauer CK, Stella L, Ciolfi A, Aawi M, et al. Mutations in KCNH1 and ATP6V1B2 cause Zimmermann-Laband syndrome. Nat Genet 2015; 47: 661–7.

Lemke JR, Riesch E, Scheurenbrand T, Schubach M, Wilhelm C, Steiner I, et al. Targeted next generation sequencing as a diagnostic tool in epileptic disorders. Epilepsia 2012; 53: 1387–98.

Machnicka B, Czogalla A, Hryniewicz-Jankowska A, Boguslawska DM, Grochowalska R, Heger E, et al. Spectrins: a structural platform for stabilization and activation of membrane channels, receptors and transporters. Biochim Biophys Acta 2014; 1838: 620–34.

Michalczyk I, Toporkiewicz M, Dubielecka PM, Chorzalska A, Sikorski AF. PKC-theta is a negative regulator of TRAIL-induced and FADD-mediated apoptotic spectrin aggregation. Folia Histochem Cytobiol 2016; 54: 1–13.

Nonoda Y, Saito Y, Nagai S, Sasaki M, Iwasaki T, Matsumoto N, et al. Progressive diffuse brain atrophy in West syndrome with marked hypomyelination due to SPTAN1 gene mutation. Brain Dev 2013; 35: 280–3.

Pettersen EF, Goddard TD, Huang CC, Couch GS, Greenblatt DM, Meng EC, et al. UCSF Chimera–a visualization system for exploratory research and analysis. J Comput Chem 2004; 25: 1605–12.

Ream MA, Mikati MA. Clinical utility of genetic testing in pediatric drug-resistant epilepsy: a pilot study. Epilepsy Behav 2014; 37: 241–8.

Retterer K, Juusola J, Cho MT, Vitazka P, Millan F, Gibellini F, et al. Clinical application of whole-exome sequencing across clinical indications. Genet Med 2016; 18: 696–704.

Richards S, Aziz N, Bale S, Bick D, Das S, Gastier-Foster J, et al. Standards and guidelines for the interpretation of sequence variants: a joint consensus recommendation of the American College of Medical Genetics and Genomics and the Association for Molecular Pathology. Genet Med 2015; 17: 405–24.

Saitsu H, Kato M, Mizuguchi T, Hamada K, Osaka H, Tohyama J, et al. *De novo* mutations in the gene encoding STXBP1 (MUNC18-1) cause early infantile epileptic encephalopathy. Nat Genet 2008; 40: 782–8.

Saitsu H, Nishimura T, Muramatsu K, Kodera H, Kumada S, Sugai K, et al. *De novo* mutations in the autophagy gene WDR45 cause static encephalopathy of childhood with neurodegeneration in adulthood. Nat Genet 2013; 45: 445–9.

Saitsu H, Tohyama J, Kumada T, Egawa K, Hamada K, Okada I, et al. Dominant-negative mutations in alpha-II spectrin cause west syndrome with severe cerebral hypomyelination, spastic quadriplegia, and developmental delay. Am J Hum Genet 2010; 86: 881–91.

Schwede T, Kopp J, Guex N, Peitsch MC. SWISS-MODEL: an automated protein homology-modeling server. Nucleic Acids Res 2003; 31: 3381–5.

Stavropoulos DJ, Merico D, Jobling R, Bowdin S, Monfared N, Thiruvahindrapuram B, et al. Whole-genome sequencing expands diagnostic utility and improves clinical management in paediatric medicine. NPJ Genom Med 2016; 1: 15012.

Susuki K, Raphael AR, Ogawa Y, Stankewich MC, Peles E, Talbot WS, et al. Schwann cell spectrins modulate peripheral nerve myelination. Proc Natl Acad Sci USA 2011; 108: 8009–14.

Tohyama J, Akasaka N, Osaka H, Maegaki Y, Kato M, Saito N, et al. Early onset West syndrome with cerebral hypomy elination and reduced cerebral white matter. Brain Dev 2008; 30: 349–55.

Tohyama J, Nakashima M, Nabatame S, Gaik-Siew C, Miyata R, Rener-Primec Z, et al. SPTAN1 encephalopathy: distinct phenotypes and genotypes. J Hum Genet 2015; 60: 167–73.

Tzschach A, Grasshoff U, Schaferhoff K, Bonin M, Dufke A, Wolff M, et al. Interstitial 9q34.11-q34.13 deletion in a patient with severe intellectual disability, hydrocephalus, and cleft lip/palate. Am J Med Genet A 2012; 158 A: 1709–12.

Ursitti JA, Kotula L, DeSilva TM, Curtis PJ, Speicher DW. Mapping the human erythrocyte beta-spectrin dimer initiation site using recombinant peptides and correlation of its phasing with the alpha-actinin dimer site. J Biol Chem 1996; 271: 6636–44.

Voas MG, Lyons DA, Naylor SG, Arana N, Rasband MN, Talbot WS. alpha II-spectrin is essential for assembly of the nodes of Ranvier in myelinated axons. Curr Biol 2007; 17: 562–8.

Writzl K, Primec ZR, Strazisar BG, Osredkar D, Pecaric-Meglic N, Kranjc BS, et al. Early onset West syndrome with severe hypomyelination and coloboma-like optic discs in a girl with SPTAN1 mutation. Epilepsia 2012; 53: e106–10.

Yan XX, Jeromin A, Jeromin A. Spectrin Breakdown Products (SBDPs) as potential biomarkers for neurode ge nerative diseases. Curr Transl Geriatr Exp Gerontol Rep 2012; 1: 85–93.

Yavarna T, Al-Dewik N, Al-Mureikhi M, Ali R, Al-Mesaifri F, Mahmoud L, et al. High diagnostic yield of clinical exome sequencing in Middle Eastern patients with Mendelian disorders. Hum Genet 2015; 134: 967–80.